

ClimbingCap: Multi-Modal Dataset and Method for Rock Climbing in World Coordinate

Ming Yan^{1,2,3*} Xincheng Lin^{1,3*} Yuhua Luo^{1,3} Shuqi Fan^{1,3} Yudi Dai⁷ Qixin Zhong⁴
 Lincui Zhong⁵ Yuexin Ma⁶ Lan Xu⁶ Chenglu Wen^{1,3} Siqi Shen^{1,3†} Cheng Wang^{1,3}

¹Fujian Key Laboratory of Sensing and Computing for Smart Cities, Xiamen University

²National Institute for Data Science in Health and Medicine, Xiamen University

³Key Laboratory of Multimedia Trusted Perception and Efficient Computing, Ministry of Education of China, School of Informatics, Xiamen University

⁴China National Climbing Team ⁵Ningbo Sports Work Training Team

⁶ShanghaiTech University ⁷ETH AI Center, ETH Zürich

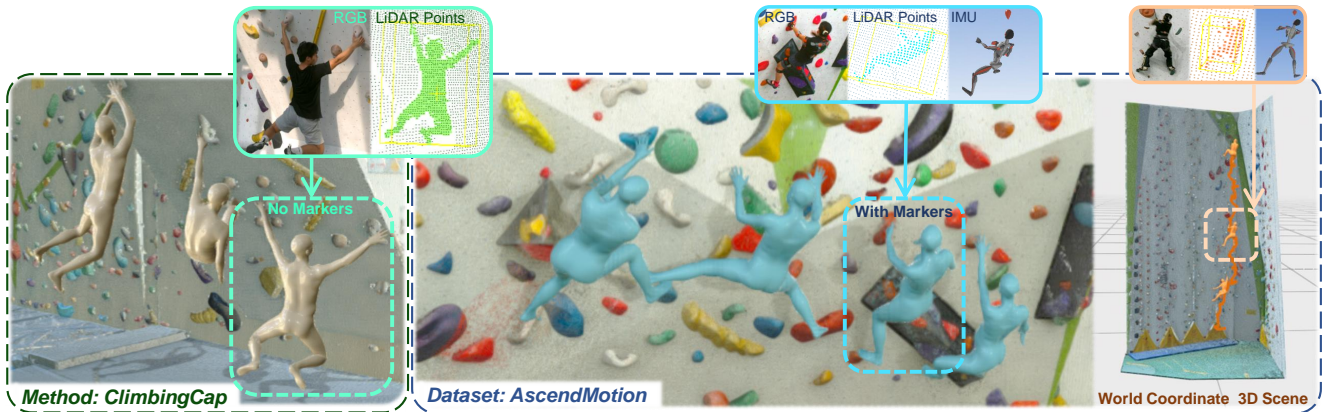


Figure 1. **Overview.** To address the challenging problem of global climbing motion recovery, we collect the dataset **AscendMotion**, using LiDAR, RGB camera and Inertial Measurement Unit (IMU) motion capture system with accurate motion labels and global trajectories (the blue and orange human bodies in right side of the figure represent labeled motions, and the orange curve represents the motion trajectory in the world coordinate.). Meanwhile, we propose **ClimbingCap**, a global climbing motion capturing method in world coordinate. As shown in the left part of this figure, it uses both image and LiDAR point cloud to recover human motions.

Abstract

*Human Motion Recovery (HMR) research mainly focuses on ground-based motions such as running. The study on capturing climbing motion, an off-ground motion, is sparse. This is partly due to the limited availability of climbing motion datasets, especially large-scale and challenging 3D labeled datasets. To address the insufficiency of climbing motion datasets, we collect **AscendMotion**, a large-scale well-annotated, and challenging climbing motion dataset. It consists of 412k RGB, LiDAR frames, and IMU measurements, including the challenging climbing motions of 22 skilled climbing coaches across 12 different rock walls. Capturing the climbing motions is challenging as it requires precise recovery of not only the complex pose but also the global position of climbers. Although multi-*

*ple global HMR methods have been proposed, they cannot faithfully capture climbing motions. To address the limitations of HMR methods for climbing, we propose **ClimbingCap**, a motion recovery method that reconstructs continuous 3D human climbing motion in a global coordinate system. One key insight is to use the RGB and LiDAR modalities to separately reconstruct motions in camera coordinates and global coordinates and to optimize them jointly. We demonstrate the quality of the AscendMotion dataset and present promising results from ClimbingCap. The AscendMotion dataset and source code release publicly at <http://www.lidarhumanmotion.net/climbingcap/>*

1. Introduction

It is challenging for global Human Motion Recovery (HMR) [1, 9, 40, 42, 80] due to the complexity of human poses and dynamic interaction between humans and their environments. Moreover, global HMR must main-

* Equal contribution.

† Corresponding author.

tain consistency in world coordinates to ensure authenticity and physical feasibility. The research community has proposed various methods to estimate human poses from different sensors such as RGB images [21–23, 33, 71], LiDAR point clouds [36, 49, 78], and inertial measurement units (IMUs) [25, 76]. Most of the studies [8, 15, 16, 24, 28, 39, 49, 62, 68, 73, 78] focus on recovering ground-based motions such as running, interacting, and dancing.

Unlike ground-based motions such as running, climbing is an activity performed off-ground, where climbers use hands and feet to ascend holds or walls. As an important sport and recreation, the climbing race has become an official event in the Olympic Games. Yet, research on climbing motion capture [26, 34, 35, 54, 61] is sparse, partly due to the limited availability of climbing datasets. There are only two publicly available climbing datasets: SPEED21 [19] and CIMI4D [72]. SPEED21 is a 2D dataset. Although CIMI4D is 3D, it consists of many trivial climbing motions from casual climbers. Moreover, the size of the two datasets is small. As a result, the research community lacks an in-depth understanding of challenging climbing motions.

We collect **AscendMotion**, a large-scale and challenging climbing motion multi-modal dataset, to address the data insufficiency. AscendMotion dataset includes the motions of 22 skilled climbers climbing 12 different rock walls. It includes rich modalities from hardware time-synchronized RGB, LiDAR point clouds, and Inertial Measurement Unit(IMU) MoCap system. Moreover, it consists of the global trajectories of climbers, which are important for understanding human motions in world coordinates. We also combine automatic annotation with manual refinement to ensure the accuracy of the motion annotation.

Not only does climbing motion challenge humans, but capturing climbing motion is also challenging for researchers. Capturing climbing motion requires precise estimation of the complex pose resulting from human-scene interactions, as well as the global localization of climbers within scenes. Existing research dedicated to climbing [8, 62, 68] uses standard 2D HMR (e.g. OpenPose [9]) for climbing motions, which is suboptimal. Most existing HMR methods [20, 37, 55, 56, 60, 75] focus on recovering ground-based human motions through RGB imagery. The estimation results of these methods cannot be rigidly transformed among camera coordinates and global coordinate systems, due to the inherent ambiguity between coordinate systems. Moreover, global HMR methods often accumulate errors during long-term sequence recovery, affecting the accuracy of global trajectories and postures, especially in climbing movements, as we show through experiments.

To tackle the above challenges and fill the gap in the motion capture community for climbing motions, we introduce **ClimbingCap**, an HMR method that reconstructs continuous 3D human climbing motion in both camera and

global coordinate systems (see Fig.1). We adopt a trilogy in ClimbingCap: separate coordinate decoding, post-processing, and semi-supervised training. For the separate coordinate decoding stage, ClimbingCap uses image and point cloud modality to estimate poses in the camera and the global coordinate systems, respectively. The post-processing stage accurately ensures the consistency of motions between the two coordinate systems. In the semi-supervised training stage, a teacher-student training method is adopted to make use of easily obtainable unlabeled climbing data. Through these innovations, we can handle complex climbing movements effectively. To summarize, our main contributions include:

- We collect the dataset AscendMotion, which is more comprehensive than existing datasets. We demonstrate the quality of the dataset and its poses are challenging.
- We propose ClimbingCap, which is a multimodality global HMR method for rock climbing.
- We conduct extensive experiments on evaluate the ClimbingCap in multiple datasets with various state-of-the-art methods. The experimental results show ClimbingCap perform better than all the methods for climbing motions.

2. Related Work

Camera-Space HMR. Camera-space HMR methods [7, 12, 13, 18, 27, 30, 31, 38, 44, 46, 48, 52, 53, 57–59, 63, 65, 70, 74, 81] predict human motion in independent camera coordinate system for each frame of the input video. Although camera-space methods can predict accurate human poses, they cannot effectively reflect the orientation and trajectory of the human body in world coordinates.

World-Grounded HMR. Recent studies [32, 37, 55, 56, 60, 75, 77] have achieved remarkable progress in world coordinates. Most of them are two-stage methods. The first stage estimates human motion in camera coordinates, and the second stage optimizes the motion in world coordinates with the scene information. Most global HMR methods focus on ground-based motions (e.g., walking) that are located on the ground. They cannot accurately model climbing motions, which is an off-ground motion. Our method, ClimbingCap, is a global HMR method developed for recovering rock climbing motions.

HMR Dataset. We have compared the AscendMotion dataset with multiple recent datasets in Table Tab. 1. Most of the datasets focus on ground-based human daily activities or sports. There exist only two public available climbing motion datasets. SPEED21 [19] collects 2D motions of climbers from sports videos. CIMI4D [72] contains 3D motions and global trajectories of climbers. Our climbing dataset, AscendMotion (344 minutes labeled data and 441 minutes unlabeled data, 412k frames), is significantly larger than both SPEED21 (21 minutes, 46k frames) and CIMI4D

Dataset	Sensor Modalities			Global Trajectory	Frames	3D Scene	Motion	Real/Synthetic	Seqs	Subjects	Career
	RGB	MoCap	LiDAR								
SLOPER4D [15]	✓	IMU	✓	✓	100k	✓	Daily	Real	15	12	Normal
EMDB[28]	✓	EM	-	✓	105k	-	Daily	Real	81	10	Normal
BEHAVE [5]	✓	-	-	✓	15k	-	Interactions	Real	-	8	Normal
RICH [24]	✓	-	-	✓	577k	✓	Interactions	Real	142	22	Normal
AGORA [45]	✓	-	-	✓	106.7k	✓	Daily	Synthetic	-	-	-
BEDLAM [6]	✓	-	-	-	1M	✓	Daily	Synthetic	-	-	-
FreeMotion [49]	✓	IMU	✓	✓	578k	-	Daily	Real	-	-	Normal
HmPEAR [39]	✓	-	✓	-	300k	-	Daily	Real	6k	25	Normal
RELI11D [73]	✓	IMU	✓	✓	239k	✓	Sport	Real	48	10	Normal
HiSC4D [16]	✓	IMU	✓	✓	36k	✓	Sport	Real	8	-	Normal
LiDARHuman51M [78]	✓	IMU	✓	-	374k	-	Daily	Real	52	10	Normal
CIMI4D [72]	✓	IMU	✓	✓	180k	✓	Climbing	Real	42	12	Normal
SPEED21 [19]	✓	-	-	-	46k	-	Climbing	Real	95	-	-
AscendMotion(Ours)	✓	IMU	✓	✓	412k	✓(12)	Climbing	Real	220	22	Skilled

Table 1. Comparisons with related HMR datasets. The “-” symbol indicates that it is not included in the dataset.

(120 minutes, 180k frames). Moreover, the motions in our dataset are more challenging than those in CIMI4D, as they come from climbing coaches who are more skilled than the casual climbers in CIMI4D.

Climbing Motion Recovery. In recent years, the increasing popularity of climbing, coupled with the inclusion of rock climbing races in the Olympic Games, has led to growing interest in the capture and analysis of climbing motions [2, 3, 10, 51, 67]. Research on climbing MoCap methods remains limited. [43] employs OpenPose [9] for climbing pose estimation. [50] performs RGB-based method for local pose and estimates climbing position through a marker-based method.

3. Method: ClimbingCap

Climbing motion capture is challenging, involving poses with extreme limb extension and full-body exertion in camera coordinates. Moreover, it requires precise alignment with the rock wall in world coordinate as climbers are ascending. The ClimbingCap pipeline consists of three parts: separate coordinate decoding, post-processing, and semi-supervised training. An overview of the proposed pipeline is shown in Fig. 2. The separate coordinate decoding and post-processing parts take into account the unique challenges posed by climbing motion, which involves complex off-ground dynamics and interactions with scenes. The semi-supervised training part makes use of the large-scale unlabeled climbing motion data to learn better a HMR model.

3.1. Separate Coordinate Decoding

The separate coordinate decoding (SCD) stage extracts features from the RGB sequence and LiDAR point clouds, and

predicts the poses in camera coordinates and the positions in global coordinates.

Input and Feature Extraction. The overall network structure is illustrated in Fig. 2. The input includes RGB images and point cloud data. First, the point cloud data is transformed from the world coordinate system to the camera coordinate system via an extrinsic matrix, represented as $\mathcal{P}_c = \Omega_{w2c} \cdot \mathcal{P}_w$. Subsequently, the RGB images and transformed point cloud data are passed through feature extraction modules, *RGB Extract* and *PC Extract*, to obtain visual and geometric features. We build the feature extraction modules based on ViT [17] and PointNet++ [47]. These features are then fed into the following two decoder modules, which regress the SMPL parameters and global motion parameters of the human body, respectively.

Camera Coordinate Decoder. This module decodes the SMPL parameters in the camera coordinate system. The RGB and point cloud features serve as inputs to the *Camera Coordinate Decoder* (denoted as $\mathcal{T}_{\text{Decoder}}$), which processes the inputs with contextual information $\mathbf{f}_{\text{backbone}}$, generating an output token \mathbf{t}_{out} . This output token is then used to iteratively optimize the SMPL parameters, including the pose θ , shape β , and camera translation Δc . The iterative decoding approach allows the model to gradually approximate the true pose and shape in the camera coordinate system. In each iteration, the decoder updates the current SMPL parameters θ_i , β_i , and Δc_t as follows:

$$\mathbf{t}_{\text{out}} = \mathcal{T}_{\text{Decoder}}(\mathbf{t}, \mathbf{f}_{\text{backbone}}), \quad (1)$$

where $\theta_{i+1} = \Phi_{\theta} \cdot \mathbf{t}_{\text{out}} + \theta_i$, $\beta_{i+1} = \Phi_{\beta} \cdot \mathbf{t}_{\text{out}} + \beta_i$, and $\Delta c_{i+1} = \Phi_c \cdot \mathbf{t}_{\text{out}} + \Delta c_i$ are the update equations, with Φ_{θ} , Φ_{β} , and Φ_c representing the respective weight matrices for each parameter. Here, the input token \mathbf{t} can include initialized pose, shape, and camera parameters as needed.

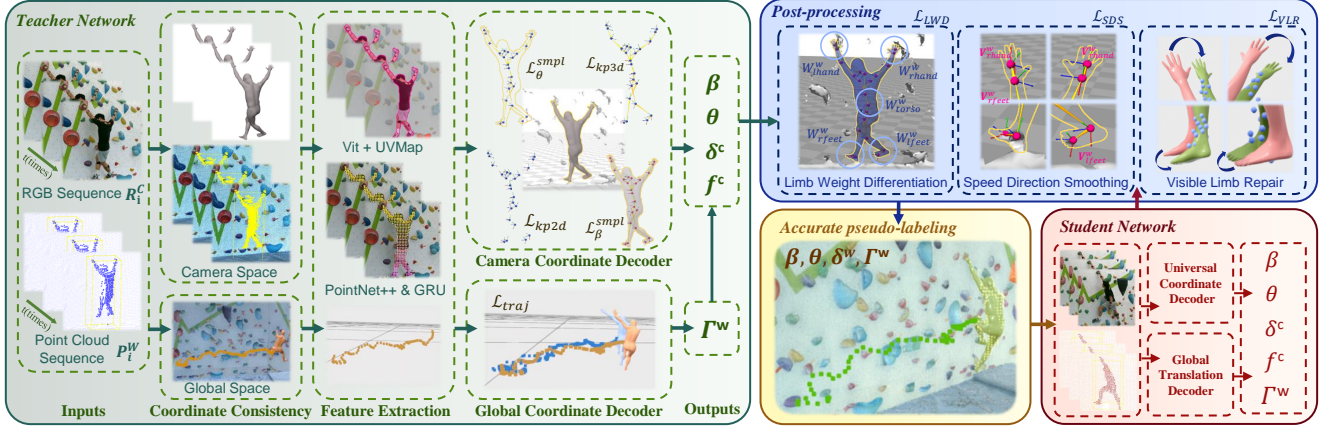


Figure 2. **Overview of ClimbingCap.** The arrows indicate the three stages of the ClimbingCap framework: separate coordinate decoding(the green box), post-processing(the blue box), and semi-supervised training(the red box).

Global Coordinate Decoder. To fully capture the human motion trajectory in the world coordinate, we design the *Global Translation Decoder* to predict the global translation parameters Γ^{trans} of the human body. In this module, the decoder processes the features $\mathbf{f}_{\text{backbone}}$ as contextual input, iteratively updating the global translation parameters. The update formula in each iteration is given by:

$$\Gamma_{i+1}^{\text{trans}} = \Psi \cdot \mathbf{t}_{\text{out}} + \Gamma_i^{\text{trans}}, \quad (2)$$

where Γ_i^{trans} represents the global translation parameters at time step i , and Ψ is the weight matrix for the update. This decoding process enables the model to capture a complete motion trajectory in the global coordinate system.

Loss. The total loss function not only includes the 3D keypoint loss $\mathcal{L}_{\text{kp3d}}$ and 2D keypoint loss $\mathcal{L}_{\text{kp2d}}$ but also incorporates the SMPL parameter loss $\mathcal{L}^{\text{smpl}}$ and the global trajectory loss $\mathcal{L}_{\text{traj}}$. Specifically, the 3D keypoint loss $\mathcal{L}_{\text{kp3d}}$ measures the 3D error of the predicted keypoints, while the 2D keypoint loss $\mathcal{L}_{\text{kp2d}}$ measures the 2D projection error. The SMPL parameter loss $\mathcal{L}^{\text{smpl}}$ supervises the decoded pose and shape parameters, and the global trajectory loss $\mathcal{L}_{\text{traj}}$ constrains the translation parameters to within close distance of ground truth positions. Please see the supplementary for details. The final total loss is formulated as:

$$\mathcal{L} = \mathcal{L}_{\text{kp3d}} + \mathcal{L}_{\text{kp2d}} + \mathcal{L}_{\theta}^{\text{smpl}} + \mathcal{L}_{\beta}^{\text{smpl}} + \mathcal{L}_{\text{traj}}. \quad (3)$$

3.2. Post-processing

Researches [55, 56, 75] have shown that a post-processing stage can be used to improve the output motion recovery results. Following these approaches, we employ a post-processing stage to optimize the output pose from SCD 3.1 stage.

One distinct advantage of ClimbingCap is that the output results for the pose decoding stage can be rigidly transformed between the camera coordinate system and the world coordinate system. Thanks to the LiDAR modality, the point cloud contains 3D information in the world coordinate system. The poses obtained from the SCD stage are converted from the camera coordinate system to the world coordinate system through the inverse extrinsic matrix Ω_{w2c}^{-1} .

The post-processing stage consists of three losses: \mathcal{L}_{LWD} , \mathcal{L}_{SDS} , and \mathcal{L}_{VLR} . \mathcal{L}_{LWD} assigns different weights to the vertices of different parts of the climbing human SMPL, and optimizes the position of the human body in the world coordinate system according to these weights. \mathcal{L}_{SDS} optimizes joint positions by smoothing the changes in the direction of the human body’s velocity on the scene (i.e., rock wall). \mathcal{L}_{VLR} optimizes the difficult-to-estimate limb end poses by using the position of the point cloud in space. In this stage, the global poses are optimized through using the Adam [29] optimizer. Please refer to the supplementary for detailed definition of these losses.

3.3. Semi-supervised Training

Compared to ground-based motions [41], the size of labeled climbing motions is small. Simply using labeled climbing motion data may not be enough to train a robust model. Different from labeled climbing motion data, collecting unlabeled climbing motion data is cheaper. The AscendMotion dataset contains more unlabeled data than label data. They can be used to further improve the HMR model.

It has been shown by researches [64, 69, 79] from the object detection community that through using a teacher-student semi-supervised training framework, the performance of object detection models can be improved. We adopt such semi-supervised training frame for HMR. In this work, we refer the model trained after the SCD and the post-



Figure 3. Dataset collection hardware system.

processing stage as the teacher model (green box in Fig. 2). The student model (red box in Fig. 2) clones the parameters of the teacher model. During semi-supervised training, the teacher model estimate the pose labels from unlabeled motion data, and the pose label is used as pseudo-label to further train the student model. We show in the experiment section that via utilizing the semi-supervised training framework, the performance of HMR can be further improved. Please refer to the supplementary for the detailed training process.

4. The AscendMotion Dataset

To advance research in Human Mesh Recovery (HMR) for climbing motion within a global coordinate system, we present the AscendMotion dataset. This dataset specifically captures complex multi-directional rock climbing motions on non-planar surfaces. It provides a unique opportunity for challenging HMR research. AscendMotion includes multi-modal motion data from skilled climbers performing various climbing styles, such as bouldering, speed climbing, and lead climbing, with synchronized recordings from IMU, RGB cameras, and LiDAR. The dataset comprises 344 minutes (6 hours) of labeled data and 441 minutes of unlabeled data, featuring 22 adult climbers across 12 real-world climbing scenes. All participants agreed to use their recorded data for scientific purposes.

4.1. Hardware and Configuration

The AscendMotion data collection system integrates multiple sensors and captures motion data in both indoor and outdoor environments. As shown in Fig. 3, the LiDAR (Ouster-OS1, 128 beams) captures 3D dynamic point clouds at 20 frames per second (FPS), while the Hik 1080P RGB camera records RGB video at 20 FPS. For each climbing environment, we use the Trimble X7 3D laser scanner to reconstruct high-resolution RGB point cloud scenes, each containing approximately 80 million points. For the labeled

dataset, each climber wears an Xsens MVN inertial motion capture system with 17 IMUs, recording at 60 FPS. [4] and a handheld point cloud scanner to ensure accurate body shape representation. For the unlabeled dataset, climbers do not wear a MoCap outfit, and we record their climbing motions using a RGB camera and a LiDAR. A human motion is represented by $M = (T, \theta, \beta)$, where T represents global translation, θ is the SMPL [40] pose parameters, and β is the SMPL shape parameter. We obtain each climber’s shape parameters β using IPNet [4].

4.2. Annotation Pipeline

The pose θ and the translation T obtained from the IMU measurements may be inaccurate. Especially the translation T may significantly drift for long-duration capture. The annotation pipeline of AscendMotion is used to find the accurate translate T and pose θ as labels.

The annotation pipeline of AscendMotion is depicted in Fig. 4. It consists of three parts: preprocessing, multi-stage global optimization, and manual annotation. The preprocessing part is used for time synchronization and spatial calibration. The multi-stage global optimization part is developed for automatic generation of annotation labels. The manual annotation part is used to further improve the quality of generated annotations.

4.2.1 Multi-modal Data Preprocessing Stage

Time Synchronization. The time among RGB camera and LiDAR is synchronized via Precision Time Protocol (PTP). We employ CollShark Auto 66 unit as the master clock, and it sends PTP slave clocks to the RGB camera and LiDAR. The time of IMU MoCap is post-synchronized with the LiDAR and RGB through anchor frames.

Calibration. First, the LiDAR point cloud are registered with high-precision scanned-scenes. Next, the coordinate of LiDAR is treated as the world coordinate. The IMU measurements are transformed into the world coordinate through a calibration matrix. Finally, we perform frame-level calibration among RGB, LiDAR and IMU. Please refer to the appendix for details.

4.2.2 Multi-stage Global Optimization

AscendMotion uses the translation T and pose θ provided by the IMU MoCap as the initialization of annotation labels, and performs multi-stage global optimization. To achieve accurate and natural human motion data consistent with the scene, we apply two loss functions: the Global Refit Loss \mathcal{L}_{GR} and the Scene Touch Loss \mathcal{L}_{ST} .

Global Refit Loss \mathcal{L}_{GR} . The global refit loss promotes precise global alignment between the SMPL model and the

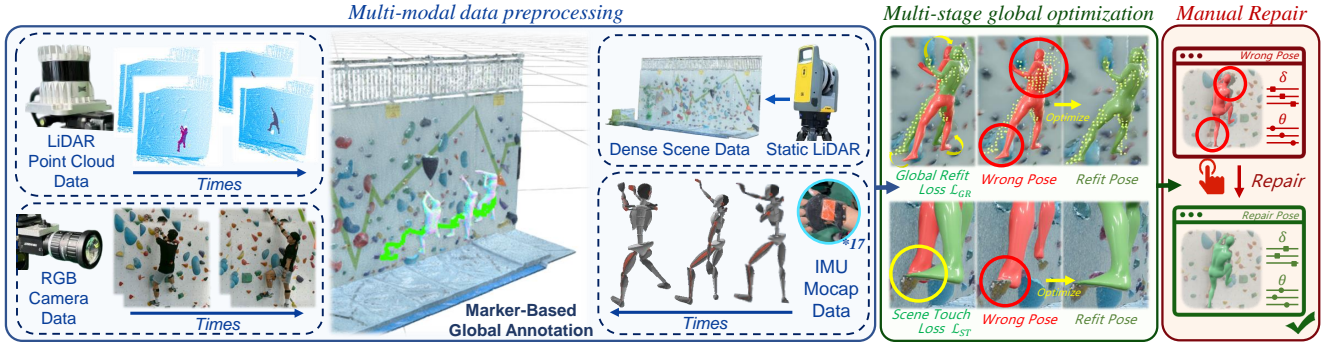


Figure 4. **AscendMotion Annotation Pipeline.** From left to right, this pipeline represents the three stages of dataset annotation: time-space synchronous input pre-processing (the blue box), multi-stage global optimization (the green box), and manual repair (the red box).

point clouds. \mathcal{L}_{GR} calculates the geometric discrepancy between the SMPL model vertices V and the human body point cloud P using a modified Chamfer distance. It applies different loss terms ($f(|v_i - p_j|^2)$ or $g(|v_i - p_j|^2)$) to different body parts to make body regions, such as the torso and limbs, match the point clouds of the human. We calculate the Euclidean distance between a vertex $v_i \in V$ and a point $p_j \in P$ as d_{v_i, p_j} . A loss term $f(|v_i - p_j|^2)$ is applied to a vertex v_i if $d_{v_i, p_j} \leq d_{\text{torso}}$, and $g(|v_i - p_j|^2)$ is applied to v_i if $d_{v_i, p_j} \leq d_{\text{limb}}$, where d_{torso} and d_{limb} are the distance thresholds for torso and limbs, respectively. During climbing, humans use limbs to climb up, the distance among limbs and scenes should smaller than the distance among torso and scenes, $d_{\text{limb}} \leq d_{\text{torso}}$.

Scene Touch Loss \mathcal{L}_{ST} . This loss prevents unrealistic intersections between the SMPL model and the scene mesh by measuring the penetration depth between the SMPL vertices $v_i \in V$ and the scene mesh vertices $q_j \in Q$. Given the scene mesh normal vectors n_j , the penetration depth for each vertex is calculated as the dot product $\eta(v_i) = (v_i - q_j) \cdot n_j$, where q_j is the closest mesh vertex to v_i . If the penetration depth $\eta(v_i)$ is negative, it indicates that the vertex v_i has penetrated the scene mesh, and this value contributes to the loss \mathcal{L}_{ST} . This loss encourages the SMPL model to avoid intersecting with the scene mesh, promoting more realistic interactions between the model and the environment.

4.2.3 Manual Annotation and Verification

To further improve the dataset quality, we use the SMPL annotation tool [66] for enhanced labeling of sequences. We engage four observers to review the automatically annotated results. For any ambiguous limb movements observed in RGB views, we perform additional manual adjustments and mark these frames as key frames. Finally, we propagate poses from multiple key frames within each sequence to ensure global consistency in both smoothness and accuracy.

Constraint term		Horizontal Scene			Vertical Scene		
\mathcal{L}_{ST}	\mathcal{L}_{GR}	ACCEL↓	MPJPE↓	PA-MPJPE↓	ACCEL↓	MPJPE↓	PA-MPJPE↓
✓	✗	1.83	37.57	32.52	6.79	51.51	46.24
✓	✗	1.67	35.45	31.81	3.73	40.36	35.37
✗	✓	1.59	29.04	25.95	1.66	29.24	24.99
✓	✓	1.54	28.20	23.25	1.60	29.07	24.37

Table 2. Quantitative Evaluation of Dataset Quality.

5. EXPERIMENTS

In this section, we demonstrate the high-quality of the AscendMotion optimization process in Sec. 5.1, show that the AscendMotion dataset is challenging to existing HMR methods, and evaluate ClimbingCap and multiple HMR methods in climbing motion datasets in Sec. 5.2. We demonstrate the promising performance of ClimbingCap and shows that each component of ClimbingCap is useful through ablation study in Sec. 5.3. Please refer to the detailed experimental setup and metrics in the supplementary.

5.1. Datasets Evaluation

To quantitatively evaluate the annotation quality of AscendMotion, we divide the scene into horizontal and vertical rock walls and evaluate the performance of the global optimization stage (in Sec. 4.2.2) by comparing the generated annotations with manual annotations.

The evaluation metrics include widely used MPJPE, Procrustes Aligned MPJPE (PA-MPJPE), per vertex error (PVE), acceleration error (Accel, in units of m/s^2). These metrics are used for evaluating HMR methods as well.

To understand the impact of different constraints used in the combined optimization stage, we perform an ablation study on two different losses: \mathcal{L}_{ST} and \mathcal{L}_{GR} . Tab. 2 shows the error metrics using different loss combinations for two scenes. The error metrics are small, demonstrating the effectiveness of the global optimization pipeline and the high quality of AscendMotion.

Modality	Method	Camera Coordinate					World Coordinate				
		ACCEL↓	MPJPE↓	PA-MPJPE↓	PVE↓	PCK0.3↑	WA-MPJPE↓	W-MPJPE↓	RTE↓	Jitter↓	T-Error↓
RGB	TRACE [60]	18.68/76.79	875.56/577.60	69.21/85.81	951.52/619.93	0.06/0.09	144.33/ 385.71	254.38/703.35	14.73/26.17	115.96/521.40	2.56/6.62
	SLAHMR [75]	5.46/96.98	232.46/467.88	84.13/285.15	283.24/552.63	0.36/0.12	277.47/447.68	804.85/ 613.60	3.64 /39.39	4.91/201.33	2.81/6.54
	WHAM [56]	4.59/35.01	110.92/143.17	76.09/ 73.36	124.2/164.91	0.76/0.62	229.42/1125.77	647.70/1499.85	5.16/9.04	3.58 /40.69	1.77/ 2.49
	GVHMR [55]	4.50/26.22	107.09/124.60	60.06/80.30	118.89/151.10	0.77/0.71	105.15/1002.11	202.45/1442.50	4.09/ 7.91	6.85/ 32.71	1.48/2.54
LiDAR	LiDARCapV2 [78]	87.99/119.62	244.6/234.52	192.17/156.39	326.45/283.27	0.53/0.50	282.12/1396.42	442.12/1518.29	16.42/10.85	176.95/165.55	1.65/2.89
	LiveHPS [49]	157.87/195.23	156.5/147.31	142.19/121.76	191.87/189.30	0.64/0.70	235.4/1369.89	392.34/1506.50	13.94/10.45	279.96/358.54	2.1/6.73
LiDAR+RGB	ImmFusion [11]	108.76/74.20	473.18/464.83	254.07/179.51	533.5/529.71	0.17/0.14	324.4/1446.01	487.92/1532.88	16.52/10.86	27.03/ 14.49	1.94/3.99
	FusionPose [14]	112.08/86.44	256.81/315.93	198.55/193.83	306.22/359.68	0.36/0.42	275.02/1445.32	444.47/1532.28	16.29/10.85	92.97/80.79	2.02/6.48
	LEIR [73]	110.18/94.57	297.95/299.62	187.26/150.56	340.61/351.52	0.41/0.37	266.82/1313.09	282.31/1435.92	9.78/9.97	73.38/85.03	1.1/ 1.20
	Ours	5.17/17.25	75.45/88.92	61.73/74.50	94.89/106.42	0.91/0.78	62.95/85.26	78.99/106.95	1.57/3.12	8.3/27.75	1.07/1.29

Table 3. **HMR Comparison in the AscendMotion dataset (Horizontal Scene/Vertical Scene).** The results for the horizontal and the vertical scene are separated by “/” in each cell. ClimbingCap performs significantly than others.

Modality	Method	Camera Coordinate					World Coordinate				
		ACCEL↓	MPJPE↓	PA-MPJPE↓	PVE↓	PCK0.3↑	WA-MPJPE↓	W-MPJPE↓	RTE↓	Jitter↓	T-Error↓
RGB	TRACE [60]	57.65	488.63	98.83	685.29	0.17	365.11	608.38	28.98	27.30	4.58
	SLAHMR [75]	6.10	228.82	82.39	201.42	0.61	391.24	445.38	13.88	12.63	2.47
	WHAM [56]	9.11	184.43	94.40	191.27	0.76	321.58	430.35	32.95	9.26	3.78
	GVHMR [55]	6.98	152.56	91.13	140.19	0.60	349.17	476.90	21.54	11.63	2.26
LiDAR	LiDARCapV2 [78]	70.72	389.97	267.76	364.26	0.50	468.00	520.06	13.56	54.25	3.12
	LiveHPS [49]	72.57	190.86	148.00	225.65	0.59	412.22	524.47	12.11	50.77	3.52
LiDAR+RGB	ImmFusion [11]	68.82	322.21	232.44	435.72	0.45	465.46	586.36	13.59	14.55	3.96
	FusionPose [14]	58.54	242.20	189.92	330.09	0.53	373.46	437.88	13.54	48.30	2.01
	LEIR [73]	16.46	206.69	117.52	269.12	0.58	228.1	370.74	10.6	38.42	1.84
	Ours	5.18	84.03	60.69	99.89	0.86	228.28	261.06	8.17	8.72	1.26

Table 4. **HMR Comparison in the CIMI4D dataset.** ClimbingCap demonstrates remarkable generalization and robustness on other climbing datasets.

5.2. Comparison on Global Motion Recovery

To evaluate the performance of global HMR, we follow the motion evaluation protocols of [55, 56] and the global trajectory evaluation protocol of [15, 73]. Following WHAM [56], to calculate the world coordinate MPJPE metrics, the predicted global sequence is divided into segments of 100 frames, and each segment is aligned with the ground truth segment either to the entire segment (WA-MPJPE) or to the first two frames (W-MPJPE). Besides WA-MPJPE and W-MPJPE, the root translation error (RTE), motion jitter (Jitter, in m/s^3), relative global translation error (T-Error in m) of the entire sequence are reported.

We evaluate ClimbingCap against *nine* methods with different modalities. The global RGB methods are TRACE [60], SLAHMR [75], WHAM [56], and GVHMR [55]. The LiDAR-based methods are LiDAR-CapV2 [78] and LiveHPS [49]. The LiDAR+RGB methods are ImmFusion [11], FusionPose [14], and LEIR [73].

Results in AscendMotion. The scenes in AscendMotion are categories into horizontal and vertical scenes, based on the major direction of human motions. Vertical motions are more challenging to human and to HMR methods than horizontal motions. The experimental results are depicted in Tab. 3. The top rows depicted the results for multiple state-of-the-art RGB-based HRM methods, and the bottom rows depicted the results for state-of-the-art LiDAR and Li-

DAR+RGB based methods. In each cell of the table, the results for the horizontal and the vertical scenes are separated by “/”. For horizontal scenes, ClimbingCap performs the best in most of the metrics, especially in terms of MPJPE, WA-MPJPE and W-MPJPE. WHAM and GVHMR performs well for the camera coordinate metrics, but not in the world coordinate metrics. For the vertical scenes, ClimbingCap performs the best and significantly better than the second-best methods. GVHMR, a representative global HMR method, performs poorly in vertical scenes. It estimates the direction of movement by predicting the horizontal velocity. However, the major movement on the vertical scene of AscendMotion is an upward climbing movement. The LiDAR-based, and other LiDAR+RGB-based methods perform inferior to ClimbingCap. These methods do not fully consider global trajectories. The results demonstrate the importance of considering the relationship among camera coordinates and global coordinates.

Results in CIMI4D. To test the generalization ability of all the HMR methods, we evaluate their performance in the CIMI4D climbing dataset without retraining or fine-tuning. The CIMI4D dataset consists mostly horizontal scenes, and the motions are less challenging than AscendMotion. As it is reported in Tab. 4, ClimbingCap *performs the best in the CIMI4D dataset for most the metrics*, except the WA-MPJPE metric.



Figure 5. **Qualitative Evaluation in the AscendMotion and CIMI4D dataset.** The left and right areas show the results of Camera Coordinate and World Coordinate respectively. The red circles indicate obvious errors. The last row shows the results for CIMI4D dataset. Our method ClimbingCap performs best qualitatively by comparison.

Variant	MPJPE	PA-MPJPE	PCK0.3	WA-MPJPE	W-MPJPE	RTE
(1) RGB Input	105.67	63.05	0.78	117.17	174.53	7.64
(2) w/o \mathcal{L}_{LWD}	80.46	52.15	0.89	70.04	91.23	2.02
(3) w/o \mathcal{L}_{SDS}	99.13	60.66	0.81	109.35	164.11	7.03
(4) w/o \mathcal{L}_{VLR}	91.10	61.85	0.83	88.59	120.11	3.34
(5) w/o SS	77.43	52.57	0.90	65.30	82.09	1.83
RGB+LiDAR Input	75.45	50.51	0.91	62.95	78.99	1.57
Full Model						

Table 5. Ablation Experiment for ClimbingCap in AscendMotion.

5.3. Ablation Experiment

To understand the impact of each global loss and the semi-supervised module on ClimbingCap’s performance, we evaluate five variants of ClimbingCap on the AscendMotion dataset following the same training and evaluation protocol as the previous section. (1) RGB Input: Using only RGB imagery without LiDAR, this variant performs worst overall due to missing global position data required for post-processing. (2) w/o \mathcal{L}_{LWD} : Excluding the limb weight differentiation loss, which guides optimization using global point clouds, has a limited impact, indicating a beneficial but non-essential role. (3) w/o \mathcal{L}_{SDS} : Removing the velocity direction smoothing loss, which ensures motion consistency, significantly reduces global metrics, highlighting its importance. (4) w/o \mathcal{L}_{VLR} : The velocity direction smoothing loss constrains limb movements and corrects unexpected mis-predicted movements in a motion sequence; without this loss, ClimbingCap’s global metrics drop sig-

nificantly, highlighting its importance for consistency and accuracy. (5) w/o SS : Removing the semi-supervised module results in a slight performance decrease, indicating its contribution to improving network training, though with a modest effect. The full ClimbingCap model, with RGB and LiDAR inputs, all loss terms, and the semi-supervised framework, achieves the best results in Tab. 5, validating the design’s effectiveness for climbing motion analysis on AscendMotion.

6. Conclusion

In this work, we propose AscendMotion, a large-scale and multi-modal climbing motion dataset, and ClimbingCap, a human motion recovery framework for climbing motions. AscendMotion provides a rich, high-quality dataset that surpasses previous climbing datasets in both scale and complexity. ClimbingCap effectively recovers 3D climbing motions in the global coordinate system, ensuring accurate pose estimation and global localization. Experimental results demonstrate the quality of AscendMotion dataset, and show that ClimbingCap outperforms existing methods in terms of accuracy and robustness.

Acknowledgment. This work was partially supported by the Fundamental Research Funds for the Central Universities (No. 20720230033); by PDL (2022-PDL-12); by Xiaomi Young Talents Program.

References

- [1] Thiemo Alldieck, Marc Kassubeck, Bastian Wandt, Bodo Rosenhahn, and Marcus Magnor. Optical flow-based 3d human motion estimation from monocular video. In *German Conference on Pattern Recognition*, pages 347–360. Springer, 2017. 1
- [2] Marina Andric, Francesco Ricci, and Floriano Zini. Sensor-based activity recognition and performance assessment in climbing: A review. *IEEE Access*, 10:108583–108603, 2022. 3
- [3] Raul Beltrán Beltrán, Julia Richter, Guido Köstermeyer, and Ulrich Heinkel. Climbing technique evaluation by means of skeleton video stream analysis. *Sensors*, 23(19):8216, 2023. 3
- [4] Bharat Lal Bhatnagar, Cristian Sminchisescu, Christian Theobalt, and Gerard Pons-Moll. Combining implicit function learning and parametric models for 3d human reconstruction. In *Computer Vision—ECCV 2020: 16th European Conference, Glasgow, UK, August 23–28, 2020, Proceedings, Part II 16*, pages 311–329. Springer, 2020. 5
- [5] Bharat Lal Bhatnagar, Xianghui Xie, Ilya A Petrov, Cristian Sminchisescu, Christian Theobalt, and Gerard Pons-Moll. Behave: Dataset and method for tracking human object interactions. In *Proceedings of the IEEE/CVF Conference on Computer Vision and Pattern Recognition*, pages 15935–15946, 2022. 3
- [6] Michael J Black, Priyanka Patel, Joachim Tesch, and Jinlong Yang. Bedlam: A synthetic dataset of bodies exhibiting detailed lifelike animated motion. In *Proceedings of the IEEE/CVF Conference on Computer Vision and Pattern Recognition*, pages 8726–8737, 2023. 3
- [7] Federica Bogo, Angjoo Kanazawa, Christoph Lassner, Peter V. Gehler, Javier Romero, and Michael J. Black. Keep it simple: Automatic estimation of 3d human pose and shape from a single image. In *ECCV*, 2016. 2
- [8] Christoph Bregler and Jitendra Malik. Tracking people with twists and exponential maps. *Proceedings. 1998 IEEE Computer Society Conference on Computer Vision and Pattern Recognition (Cat. No.98CB36231)*, pages 8–15, 1998. 2
- [9] Zhe Cao, Tomas Simon, Shih-En Wei, and Yaser Sheikh. Realtime multi-person 2d pose estimation using part affinity fields. In *Computer Vision and Pattern Recognition (CVPR)*, 2017. 1, 2, 3
- [10] Kyungsik Cha, Eun-Young Lee, Myeong-Hyeon Heo, Kyu-Cheol Shin, Jonghee Son, and Dongho Kim. Analysis of climbing postures and movements in sport climbing for realistic 3d climbing animations. *Procedia Engineering*, 112: 52–57, 2015. 3
- [11] Anjun Chen, Xiangyu Wang, Kun Shi, Shaohao Zhu, Bin Fang, Yingfeng Chen, Jiming Chen, Yuchi Huo, and Qi Ye. Immfusion: Robust mmwave-rgb fusion for 3d human body reconstruction in all weather conditions. In *2023 IEEE International Conference on Robotics and Automation (ICRA)*, pages 2752–2758. IEEE, 2023. 7
- [12] Xin Chen, Anqi Pang, Wei Yang, Yuexin Ma, Lan Xu, and Jingyi Yu. Sportscap: Monocular 3d human motion capture and fine-grained understanding in challenging sports videos. *International Journal of Computer Vision*, 129:2846–2864, 2021. 2
- [13] Hai Ci, Mingdong Wu, Wentao Zhu, Xiaoxuan Ma, Hao Dong, Fangwei Zhong, and Yizhou Wang. Gfpose: Learning 3d human pose prior with gradient fields. In *CVPR*, pages 4800–4810, 2023. 2
- [14] Peishan Cong, Yiteng Xu, Yiming Ren, Juzhe Zhang, Lan Xu, Jingya Wang, Jingyi Yu, and Yuexin Ma. Weakly supervised 3d multi-person pose estimation for large-scale scenes based on monocular camera and single lidar. In *AAAI*, pages 461–469. AAAI Press, 2023. 7
- [15] Yudi Dai, Yitai Lin, XiPing Lin, Chenglu Wen, Lan Xu, Hongwei Yi, Siqi Shen, Yuexin Ma, and Cheng Wang. Sloper4d: A scene-aware dataset for global 4d human pose estimation in urban environments. In *Proceedings of the IEEE/CVF Conference on Computer Vision and Pattern Recognition*, pages 682–692, 2023. 2, 3, 7
- [16] Yudi Dai, Zhiyong Wang, Xiping Lin, Chenglu Wen, Lan Xu, Siqi Shen, Yuexin Ma, and Cheng Wang. Hisc4d: Human-centered interaction and 4d scene capture in large-scale space using wearable imus and lidar. *IEEE Transactions on Pattern Analysis and Machine Intelligence*, 2024. 2, 3
- [17] Alexey Dosovitskiy, Lucas Beyer, Alexander Kolesnikov, Dirk Weissenborn, Xiaohua Zhai, Thomas Unterthiner, Mostafa Dehghani, Matthias Minderer, Georg Heigold, Sylvain Gelly, Jakob Uszkoreit, and Neil Houlsby. An image is worth 16x16 words: Transformers for image recognition at scale. In *9th International Conference on Learning Representations, ICLR 2021, Virtual Event, Austria, May 3-7, 2021*. OpenReview.net, 2021. 3
- [18] Zhiyang Dou, Qingxuan Wu, Cheng Lin, Zeyu Cao, Qiangqiang Wu, Weilin Wan, Taku Komura, and Wenping Wang. TORE: token reduction for efficient human mesh recovery with transformer. In *ICCV*, 2023. 2
- [19] Petr Elias, Veronika Skvarlova, and Pavel Zezula. Speed21: Speed climbing motion dataset. In *Proceedings of the 4th International Workshop on Multimedia Content Analysis in Sports*, pages 43–50, 2021. 2, 3
- [20] Shubham Goel, Georgios Pavlakos, Jathushan Rajasegaran, Angjoo Kanazawa, and Jitendra Malik. Humans in 4d: Reconstructing and tracking humans with transformers. In *Proceedings of the IEEE/CVF International Conference on Computer Vision*, pages 14783–14794, 2023. 2
- [21] Marc Habermann, Weipeng Xu, Michael Zollhöfer, Gerard Pons-Moll, and Christian Theobalt. Livecap: Real-time human performance capture from monocular video. *ACM Transactions on Graphics (TOG)*, 38(2):14:1–14:17, 2019. 2
- [22] Marc Habermann, Weipeng Xu, Michael Zollhofer, Gerard Pons-Moll, and Christian Theobalt. Deepcap: Monocular human performance capture using weak supervision. In *Proceedings of the IEEE/CVF Conference on Computer Vision and Pattern Recognition (CVPR)*, 2020.
- [23] Yannan He, Anqi Pang, Xin Chen, Han Liang, Minye Wu, Yuexin Ma, and Lan Xu. Challengcap: Monocular 3d capture of challenging human performances using multi-modal refer-

- ences. In *Proceedings of the IEEE/CVF Conference on Computer Vision and Pattern Recognition*, pages 11400–11411, 2021. 2
- [24] Chun-Hao P Huang, Hongwei Yi, Markus Höschle, Matvey Safroshkin, Tsvetelina Alexiadis, Senya Polikovsky, Daniel Scharstein, and Michael J Black. Capturing and inferring dense full-body human-scene contact. In *Proceedings of the IEEE/CVF Conference on Computer Vision and Pattern Recognition*, pages 13274–13285, 2022. 2, 3
- [25] Yinghao Huang, Manuel Kaufmann, Emre Aksan, Michael J. Black, Otmar Hilliges, and Gerard Pons-Moll. Deep inertial poser: Learning to reconstruct human pose from sparse inertial measurements in real time. *ACM Transactions on Graphics, (Proc. SIGGRAPH Asia)*, 37(6):185:1–185:15, 2018. 2
- [26] Hitomi Iguma, Akihiro Kawamura, and Ryo Kurazume. A new 3d motion and force measurement system for sport climbing. In *2020 IEEE/SICE International Symposium on System Integration, SII 2020, Honolulu, HI, USA, January 12-15, 2020*, pages 1002–1007. IEEE, 2020. 2
- [27] Angjoo Kanazawa, Michael J. Black, David W. Jacobs, and Jitendra Malik. End-to-end recovery of human shape and pose. In *Computer Vision and Pattern Recognition (CVPR)*, 2018. 2
- [28] Manuel Kaufmann, Jie Song, Chen Guo, Kaiyue Shen, Tianjian Jiang, Chengcheng Tang, Juan José Zárate, and Otmar Hilliges. Emdb: The electromagnetic database of global 3d human pose and shape in the wild. In *Proceedings of the IEEE/CVF International Conference on Computer Vision*, pages 14632–14643, 2023. 2, 3
- [29] Diederik P Kingma and Jimmy Lei Ba. Adam: A method for stochastic gradient descent. In *ICLR: international conference on learning representations*, pages 1–15. ICLR US., 2015. 4
- [30] Muhammed Kocabas, Nikos Athanasiou, and Michael J. Black. Vibe: Video inference for human body pose and shape estimation. In *Proceedings of the IEEE/CVF Conference on Computer Vision and Pattern Recognition (CVPR)*, 2020. 2
- [31] Muhammed Kocabas, Chun-Hao P. Huang, Otmar Hilliges, and Michael J. Black. Pare: Part attention regressor for 3d human body estimation. In *Proceedings of the IEEE/CVF International Conference on Computer Vision (ICCV)*, pages 11127–11137, 2021. 2
- [32] Muhammed Kocabas, Ye Yuan, Pavlo Molchanov, Yunrong Guo, Michael J Black, Otmar Hilliges, Jan Kautz, and Umar Iqbal. Pace: Human and camera motion estimation from in-the-wild videos. In *2024 International Conference on 3D Vision (3DV)*, pages 397–408. IEEE, 2024. 2
- [33] Nikos Kolotouros, Georgios Pavlakos, Michael J Black, and Kostas Daniilidis. Learning to reconstruct 3d human pose and shape via model-fitting in the loop. In *Proceedings of the IEEE/CVF International Conference on Computer Vision*, pages 2252–2261, 2019. 2
- [34] Felix Kosmalla, André Zenner, Marco Speicher, Florian Daiber, Nico Herbig, and Antonio Krüger. Exploring rock climbing in mixed reality environments. In *Proceedings of the 2017 CHI Conference Extended Abstracts on Human Factors in Computing Systems*, page 1787–1793, New York, NY, USA, 2017. Association for Computing Machinery. 2
- [35] Felix Kosmalla, André Zenner, Corinna Tasch, Florian Daiber, and Antonio Krüger. The importance of virtual hands and feet for virtual reality climbing. In *Extended Abstracts of the 2020 CHI Conference on Human Factors in Computing Systems, CHI 2020, Honolulu, HI, USA, April 25-30, 2020*, pages 1–8. ACM, 2020. 2
- [36] Jialian Li, Jingyi Zhang, Zhiyong Wang, Siqi Shen, Chenglu Wen, Yuexin Ma, Lan Xu, Jingyi Yu, and Cheng Wang. Lidarcap: Long-range marker-less 3d human motion capture with lidar point clouds. In *Proceedings of the IEEE/CVF Conference on Computer Vision and Pattern Recognition*, pages 20502–20512, 2022. 2
- [37] Jiefeng Li, Ye Yuan, Davis Rempe, Haotian Zhang, Pavlo Molchanov, Cewu Lu, Jan Kautz, and Umar Iqbal. Coin: Control-inpainting diffusion prior for human and camera motion estimation. In *European Conference on Computer Vision*, pages 426–446. Springer, 2025. 2
- [38] Zhihao Li, Jianzhuang Liu, Zhensong Zhang, Songcen Xu, and Youliang Yan. Cliff: Carrying location information in full frames into human pose and shape estimation. In *ECCV*, 2022. 2
- [39] Yitai Lin, Zhijie Wei, Wanfa Zhang, Xiping Lin, Yudi Dai, Chenglu Wen, Siqi Shen, Lan Xu, and Cheng Wang. Hmpear: A dataset for human pose estimation and action recognition. In *Proceedings of the 32nd ACM International Conference on Multimedia*, pages 2069–2078, 2024. 2, 3
- [40] Matthew Loper, Naureen Mahmood, Javier Romero, Gerard Pons-Moll, and Michael J. Black. Smpl: A skinned multi-person linear model. *ACM Trans. Graph.*, 34(6):248:1–248:16, 2015. 1, 5
- [41] Naureen Mahmood, Nima Ghorbani, Nikolaus F. Troje, Gerard Pons-Moll, and Michael J. Black. Amass: Archive of motion capture as surface shapes. In *Proceedings of the IEEE/CVF International Conference on Computer Vision (ICCV)*, 2019. 4
- [42] Julieta Martinez, Rayat Hossain, Javier Romero, and James J Little. A simple yet effective baseline for 3d human pose estimation. In *ICCV*, 2017. 1
- [43] Dominik Pandurevic, Paweł Draga, Alexander Sutor, and Klaus Hochradel. Analysis of competition and training videos of speed climbing athletes using feature and human body keypoint detection algorithms. *Sensors*, 22(6):2251, 2022. 3
- [44] Chaitanya Patel, Zhouyingcheng Liao, and Gerard Pons-Moll. Tailornet: Predicting clothing in 3d as a function of human pose, shape and garment style. *2020 IEEE/CVF Conference on Computer Vision and Pattern Recognition (CVPR)*, pages 7363–7373, 2020. 2
- [45] Priyanka Patel, Chun-Hao P. Huang, Joachim Tesch, David T. Hoffmann, Shashank Tripathi, and Michael J. Black. AGORA: Avatars in geography optimized for regression analysis. In *Proceedings IEEE/CVF Conf. on Computer Vision and Pattern Recognition (CVPR)*, 2021. 3
- [46] Georgios Pavlakos, Vasileios Choutas, Nima Ghorbani, Timo Bolkart, Ahmed A. A. Osman, Dimitrios Tzionas, and

- Michael J. Black. Expressive body capture: 3d hands, face, and body from a single image. In *Proceedings IEEE Conf. on Computer Vision and Pattern Recognition (CVPR)*, pages 10975–10985, 2019. 2
- [47] Charles Ruizhongtai Qi, Li Yi, Hao Su, and Leonidas J Guibas. Pointnet++: Deep hierarchical feature learning on point sets in a metric space. *Advances in neural information processing systems*, 30, 2017. 3
- [48] Davis Rempe, Tolga Birdal, Aaron Hertzmann, Jimei Yang, Srinath Sridhar, and Leonidas J. Guibas. Humor: 3d human motion model for robust pose estimation. In *Proceedings of the IEEE/CVF International Conference on Computer Vision (ICCV)*, pages 11488–11499, 2021. 2
- [49] Yiming Ren, Xiao Han, Chengfeng Zhao, Jingya Wang, Lan Xu, Jingyi Yu, and Yuexin Ma. Livehps: Lidar-based scene-level human pose and shape estimation in free environment. In *Proceedings of the IEEE/CVF Conference on Computer Vision and Pattern Recognition*, pages 1281–1291, 2024. 2, 3, 7
- [50] Lionel Reveret, Sylvain Chapelle, Franck Quaine, and Pierre Legreneur. 3d visualization of body motion in speed climbing. *Frontiers in Psychology*, 11:2188, 2020. 3
- [51] Julia Richter, Raul Beltrán Beltrán, Guido Köstermeyer, and Ulrich Heinkel. Human climbing and bouldering motion analysis: A survey on sensors, motion capture, analysis algorithms, recent advances and applications. *VISIGRAPP (5: VISAPP)*, pages 751–758, 2020. 3
- [52] Shunsuke Saito, Zeng Huang, Ryota Natsume, Shigeo Morishima, Hao Li, and Angjoo Kanazawa. Pifu: Pixel-aligned implicit function for high-resolution clothed human digitization. In *2019 IEEE/CVF International Conference on Computer Vision, ICCV 2019, Seoul, Korea (South), October 27 - November 2, 2019*, pages 2304–2314. IEEE, 2019. 2
- [53] Shunsuke Saito, Tomas Simon, Jason M. Saragih, and Hanbyul Joo. Pifuhd: Multi-level pixel-aligned implicit function for high-resolution 3d human digitization. In *2020 IEEE/CVF Conference on Computer Vision and Pattern Recognition, CVPR 2020, Seattle, WA, USA, June 13-19, 2020*, pages 81–90. Computer Vision Foundation / IEEE, 2020. 2
- [54] Katsuhito Sasaki, Keisuke Shiro, and Jun Rekimoto. Exempose: Predicting poses of experts as examples for beginners in climbing using a neural network. In *Proceedings of the Augmented Humans International Conference, AHs 2020, Kaiserslautern, Germany, 16-17 March, 2020*, pages 18:1–18:9. ACM, 2020. 2
- [55] Zehong Shen, Huaijin Pi, Yan Xia, Zhi Cen, Sida Peng, Zechen Hu, Hujun Bao, Ruizhen Hu, and Xiaowei Zhou. World-grounded human motion recovery via gravity-view coordinates. In *SIGGRAPH Asia Conference Proceedings*, 2024. 2, 4, 7
- [56] Soyong Shin, Juyong Kim, Eni Halilaj, and Michael J Black. Wham: Reconstructing world-grounded humans with accurate 3d motion. In *Proceedings of the IEEE/CVF Conference on Computer Vision and Pattern Recognition*, pages 2070–2080, 2024. 2, 4, 7
- [57] Zhuo Su, Lan Xu, Zerong Zheng, Tao Yu, Yebin Liu, and Lu Fang. Robustfusion: Human volumetric capture with data-driven visual cues using a rgbd camera. In *ECCV*, 2020. 2
- [58] Yu Sun, Qian Bao, Wu Liu, Yili Fu, Black Michael J., and Tao Mei. Monocular, One-stage, Regression of Multiple 3D People. In *ICCV*, 2021.
- [59] Yu Sun, Wu Liu, Qian Bao, Yili Fu, Tao Mei, and Michael J Black. Putting People in their Place: Monocular Regression of 3D People in Depth. In *CVPR*, 2022. 2
- [60] Yu Sun, Qian Bao, Wu Liu, Tao Mei, and Michael J Black. Trace: 5d temporal regression of avatars with dynamic cameras in 3d environments. In *Proceedings of the IEEE/CVF Conference on Computer Vision and Pattern Recognition*, pages 8856–8866, 2023. 2, 7
- [61] Marcel Tiator, Christian Geiger, Bastian Dewitz, Ben Fischer, Laurin Gerhardt, David Nowottnik, and Hendrik Preu. Venga!: climbing in mixed reality. In *Proceedings of the First Superhuman Sports Design Challenge: First International Symposium on Amplifying Capabilities and Competing in Mixed Realities, July 2-5, 2018, Delft, The Netherlands*, pages 9:1–9:8. ACM, 2018. 2
- [62] Daniel Vlastic, Rolf Adelsberger, Giovanni Vannucci, John C. Barnwell, Markus H. Gross, Wojciech Matusik, and Jovan Popović. Practical motion capture in everyday surroundings. *ACM SIGGRAPH 2007 papers*, 2007. 2
- [63] Ziniu Wan, Zhengjia Li, Maoqing Tian, Jianbo Liu, Shuai Yi, and Hongsheng Li. Encoder-decoder with multi-level attention for 3d human shape and pose estimation. In *2021 IEEE/CVF International Conference on Computer Vision, ICCV 2021, Montreal, QC, Canada, October 10-17, 2021*, pages 13013–13022. IEEE, 2021. 2
- [64] He Wang, Yezhen Cong, Or Litany, Yue Gao, and Leonidas J Guibas. 3diomatch: Leveraging iou prediction for semi-supervised 3d object detection. In *Proceedings of the IEEE/CVF Conference on Computer Vision and Pattern Recognition*, pages 14615–14624, 2021. 4
- [65] Kuan-Chieh Wang, Zhenzhen Weng, Maria Xenochristou, João Pedro Araújo, Jeffrey Gu, Karen Liu, and Serena Yeung. Nemo: Learning 3d neural motion fields from multiple video instances of the same action. In *Proceedings of the IEEE/CVF Conference on Computer Vision and Pattern Recognition*, pages 22129–22138, 2023. 2
- [66] MeiJun Wang, Yu Meng, Zhongwei Qiu, Chao Zheng, Yan Xu, Jian Gao, et al. Pedestrian-centric 3d pre-collision pose and shape estimation from dashcam perspective. In *The Thirty-eighth Annual Conference on Neural Information Processing Systems*. 6
- [67] Emily Whiting, Nada Ouf, Liane Makatura, Christos Mousas, Zhenyu Shu, and Ladislav Kavan. Environment-scale fabrication: Replicating outdoor climbing experiences. In *Proceedings of the 2017 CHI Conference on Human Factors in Computing Systems*, pages 1794–1804. ACM, 2017. 3
- [68] HJ Woltring. New possibilities for human motion studies by real-time light spot position measurement. *Biotelemetry*, 1 (3):132, 1974. 2
- [69] Qiming Xia, Wei Ye, Hai Wu, Shijia Zhao, Leyuan Xing, Xun Huang, Jinhao Deng, Xin Li, Chenglu Wen, and Cheng

- Wang. Hinted: Hard instance enhanced detector with mixed-density feature fusion for sparsely-supervised 3d object detection. In *Proceedings of the IEEE/CVF Conference on Computer Vision and Pattern Recognition*, pages 15321–15330, 2024. 4
- [70] Yuliang Xiu, Jinlong Yang, Dimitrios Tzionas, and Michael J. Black. ICON: implicit clothed humans obtained from normals. In *IEEE/CVF Conference on Computer Vision and Pattern Recognition, CVPR 2022, New Orleans, LA, USA, June 18-24, 2022*, pages 13286–13296. IEEE, 2022. 2
- [71] Weipeng Xu, Avishek Chatterjee, Michael Zollhöfer, Helge Rhodin, Dushyant Mehta, Hans-Peter Seidel, and Christian Theobalt. Monoperfcap: Human performance capture from monocular video. *ACM Transactions on Graphics (TOG)*, 37(2):27:1–27:15, 2018. 2
- [72] Ming Yan, Xin Wang, Yudi Dai, Siqi Shen, Chenglu Wen, Lan Xu, Yuexin Ma, and Cheng Wang. Cimi4d: A large multimodal climbing motion dataset under human-scene interactions. In *Proceedings of the IEEE/CVF Conference on Computer Vision and Pattern Recognition*, pages 12977–12988, 2023. 2, 3
- [73] Ming Yan, Yan Zhang, Shuqiang Cai, Shuqi Fan, Xincheng Lin, Yudi Dai, Siqi Shen, Chenglu Wen, Lan Xu, Yuexin Ma, et al. Reli1d: A comprehensive multimodal human motion dataset and method. In *Proceedings of the IEEE/CVF Conference on Computer Vision and Pattern Recognition*, pages 2250–2262, 2024. 2, 3, 7
- [74] Ze Yang, Shenlong Wang, Siva Manivasagam, Zeng Huang, Wei-Chiu Ma, Xincheng Yan, Ersin Yumer, and Raquel Urtasun. S3: Neural shape, skeleton, and skinning fields for 3d human modeling. In *CVPR*, 2021. 2
- [75] Vickie Ye, Georgios Pavlakos, Jitendra Malik, and Angjoo Kanazawa. Decoupling human and camera motion from videos in the wild. In *IEEE Conference on Computer Vision and Pattern Recognition (CVPR)*, 2023. 2, 4, 7
- [76] Xinyu Yi, Yuxiao Zhou, Marc Habermann, Soshi Shimada, Vladislav Golyanik, Christian Theobalt, and Feng Xu. Physical inertial poser (PIP): physics-aware real-time human motion tracking from sparse inertial sensors. In *IEEE/CVF Conference on Computer Vision and Pattern Recognition, CVPR 2022, New Orleans, LA, USA, June 18-24, 2022*, pages 13157–13168. IEEE, 2022. 2
- [77] Ye Yuan, Umar Iqbal, Pavlo Molchanov, Kris Kitani, and Jan Kautz. Glamr: Global occlusion-aware human mesh recovery with dynamic cameras. In *Proceedings of the IEEE/CVF Conference on Computer Vision and Pattern Recognition (CVPR)*, 2022. 2
- [78] Jingyi Zhang, Qihong Mao, Siqi Shen, Chenglu Wen, Lan Xu, and Cheng Wang. Lidarcapv2: 3d human pose estimation with human-object interaction from lidar point clouds. *Pattern Recognition*, 156:110848, 2024. 2, 3, 7
- [79] Wu Zheng, Weiliang Tang, Li Jiang, and Chi-Wing Fu. Sssd: Self-ensembling single-stage object detector from point cloud. In *Proceedings of the IEEE/CVF conference on computer vision and pattern recognition*, pages 14494–14503, 2021. 4
- [80] Xiaowei Zhou, Menglong Zhu, Spyridon Leonardos, Konstantinos G Derpanis, and Kostas Daniilidis. Sparseness Meets Deepness: 3D Human Pose Estimation from Monocular Video. In *Computer Vision and Pattern Recognition (CVPR)*, 2016. 1
- [81] Wentao Zhu, Xiaoxuan Ma, Zhaoyang Liu, Libin Liu, Wayne Wu, and Yizhou Wang. Motionbert: Unified pretraining for human motion analysis. In *ICCV*, 2023. 2